

## Poster Presentation

### Title: Slope-unit-based assessment of landslide susceptibility in Central Nepal



In this presentation, I intend to introduce an optimised slope unit (SU) map of the Gorkha earthquake-triggered landslides affected region in central Nepal. While this work was being carried out, Tanyas et al. (2019) conducted a SU-based landslide assessment on a regional scale. The SUs used in that study were of small scale and not reasonable enough to research on a national or local scale. Therefore, a newly prepared map with well-defined optimisation criteria was necessary. The details of this work can be found in (Alvioli et al., 2022).

I also present two applications of SU maps. Firstly, a rockfall susceptibility mapping was conducted along two significant highways, Pasang Lhamu Highway and Galchhi-Rasuwegadhi Highway, in central Nepal. This work was just published on April 22, 2023 (Pokharel et al., 2023).

Secondly, I compare earthquake-triggered landslide inventories and their corresponding landslide susceptibility maps (LSMs). Both of these applications are based on slope units. The details of this work can be found in (Pokharel et al., 2021).

In the following section, I have briefly introduced slope units. I will discuss the applications presented during my sessions.

#### 1. Slope units

Availability of SU maps, an alternative to traditional pixel-based maps, aids in conducting landslide susceptibility mapping and various geomorphological studies. Since no such maps were available for the Nepal Himalayas while conducting this work, a slope unit map for central Nepal, the region significantly impacted by the Gorkha earthquake 2015, was prepared. The map was prepared following widely accepted software and methods (Alvioli et al., 2016, 2020) with a parameter-free optimisation algorithm. The methodology is discussed in *Section 2*. The map was published (Alvioli et al., 2022) in vector format with an attribute table populated with morphometric and thematic quantities for each polygon.

The delineation of SUs was performed by implementing an automatic procedure using the software *r.slopeunits* (Alvioli et al., 2016) and an enhanced optimisation strategy. This procedure uses the Shuttle radar topography mission (SRTM) elevation data at 30-m resolution. A total of 15 SRTM tiles data (N26E83, N26E84, N26E85, N26E86, N27E83, N27E84, N27E85, N27E86, N28E83, N28E84, N28E85, N28E86, N29E83, N29E84, N29E85) tiles overlapping with a polygonal area of interest (Figure 1) has been used in this work. The

Cartosat elevation data was obtained specifically for the Indian sub-continent to perform further morphometric analysis within slope units (<https://bhuvan.nrsc.gov.in>). Other data to populate the attribute table associated with the map published here, used in this study, are ancillary. The geological information was added using Hartmann & Moosdorf (2012), the presence of landslides induced by the Gorkha Earthquake of 2015 using (Pokharel et al., 2021; Roback et al., 2017), and mean daily and annual precipitation using Funk et al. (2015).

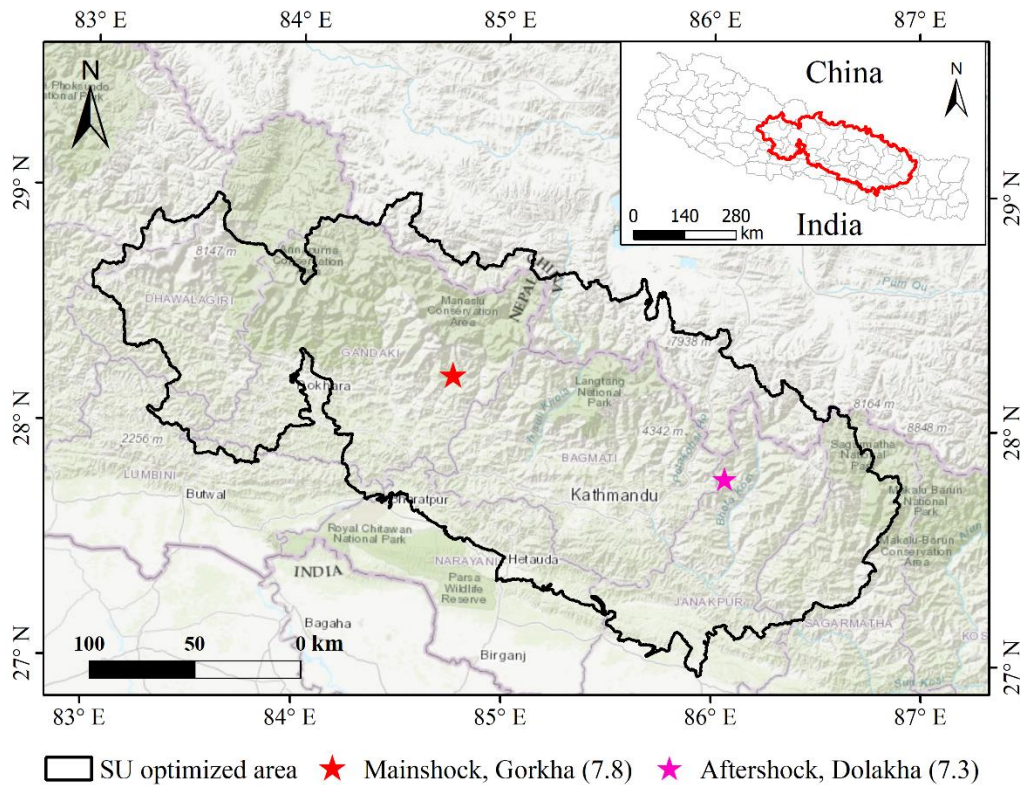


Figure 1: Map of study area, mostly central Nepal, and a small section in China.

## 2. Methodology

At first, hydrological basins for the whole area within the selected SRTM tiles were obtained, which was 1,436 basins with an area of 92.2 km<sup>2</sup>. These basins are shown as black polygons, either filled with colours or transparent in Figure 2. In this work, the basins of interest are 450 in number, which is coloured in purple. The yellow and green polygon represents the first-adjacent and the second-adjacent basins, respectively.

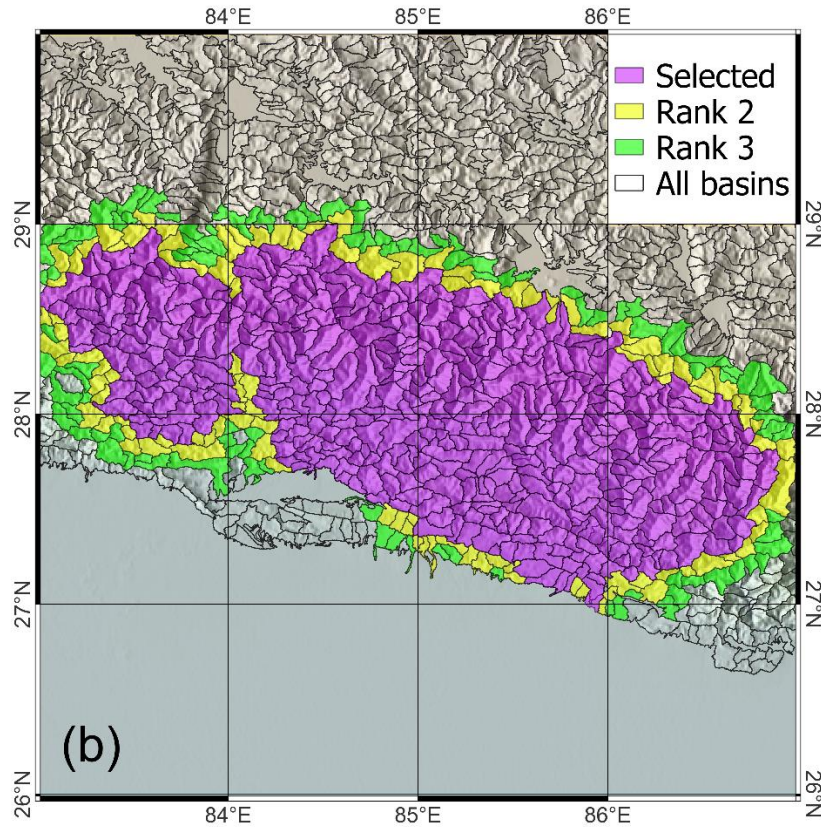


Figure 2. The map represents the extent of the 15 SRTM DEM tiles used for this study; black lines represent hydrological basins used as local domains for the slope unit delineation procedure. Purple-filled polygons are basins covering the study area. Yellow and green-filled polygons are first- and second-order basins ranked by proximity to the most peripheral purple ones.

The following sections describe the optimisation of the software's input parameters based on the ranking of basins, as mentioned above.

### ***Optimized slope unit delineation***

The software *r.slopeunits* can be considered an adaptive tool because it can delineate SU polygons of different shapes and sizes according to the local surface roughness. It is also a parametric software because adjustments for a few significant parameters are required to obtain the most suitable outputs. The key parameters that require tuning in this software are (i) minimum area,  $a_{min}$ , a tentative minimum area for output polygons, and (ii) minimum circular variance,  $c_{min}$ , representing a measure of homogeneity of each polygon in terms of slope aspect.

The optimisation procedure in this work is based on Alvioli et al. (2020) but with some modifications to remove the subjective steps. An illustration of the steps implemented in the optimisation procedure is presented in Figure 3, and these steps are described in the following.

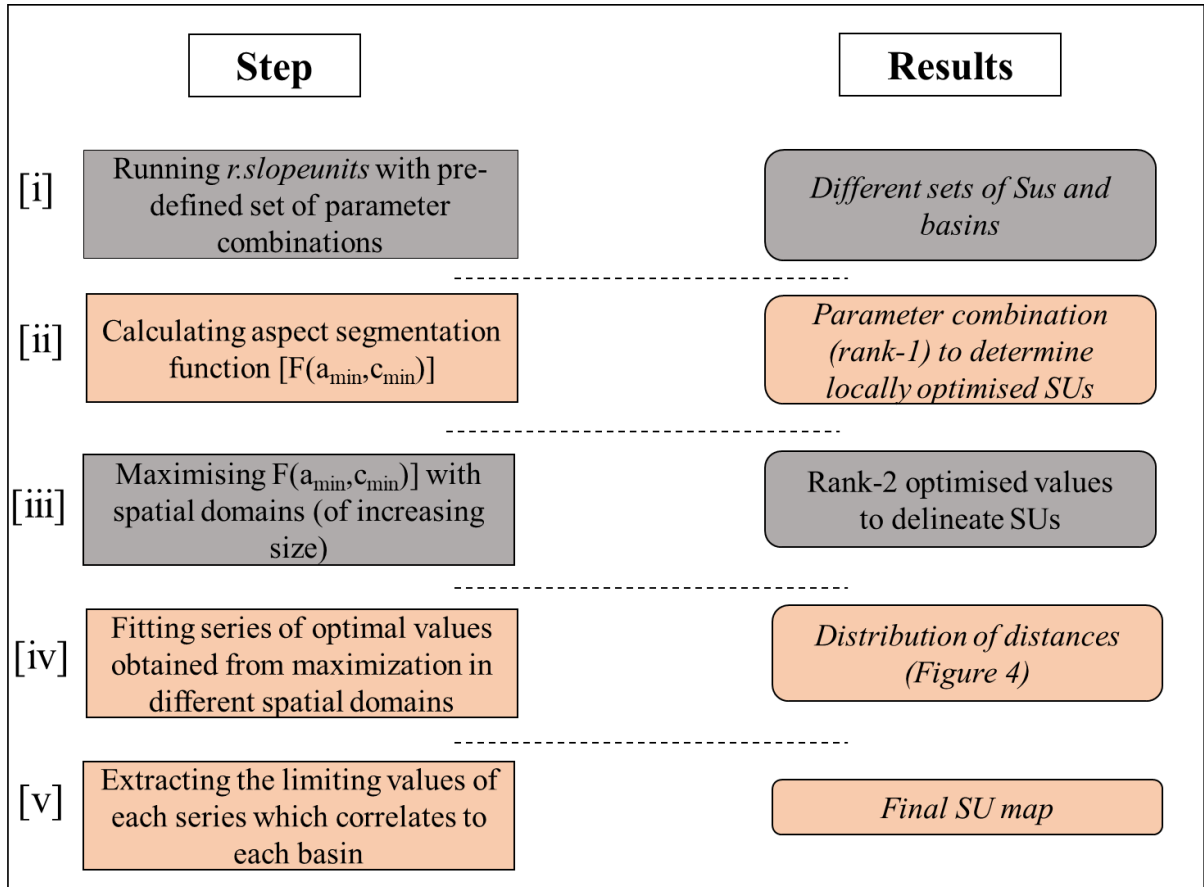


Figure 3: Flowchart of steps conducted for the optimisation procedure.

- i. The software *r.slopeunits* was run in the area of interest (coloured basins in Figure 2) for 49 combinations of key parameters ( $a_{min}$ ,  $c_{min}$ ). A grid combination between  $a_{min}$  varying in (50 k, 100 k, 150 k, 200 k, 250 k, 250 k, 300 k, 400 k)  $m^2$  and  $c_{min}$  varying in (0.01, 0.1, 0.15, 0.2, 0.3, 0.4, 0.5) produced 49 different sets of SUs for every 658 coloured basins in Figure 2.
- ii. Then, for each set of SU in the basin, the aspect segmentation function  $F(a_{min}, c_{min})$  was calculated. The function measures how well each SU map ( $(a_{min}, c_{min})$  combination) splits the topography into well-defined areas regarding terrain aspects.
- iii. Third step was to perform maximisation of  $F(a_{min}, c_{min})$  in each basin which gives the rank-1 optimal combination  $(a^{(1)_{opt}}, c^{(1)_{opt}})$ , for the basin. The optimised values spatially correlate with the values in adjacent basins. Because of this, one of the aims in this step is to find the convergence of values optimised over spatial domains of increasing size. Therefore, for each purple basin, the function  $F(a_{min}, c_{min})$  was calculated for the SU sets covered by all the neighbouring basins. From this maximisation, rank-2 optimised values of the parameters  $(a^{(2)_{opt}}, c^{(2)_{opt}})$  were obtained. From the iteration of this procedure of spatial domain expansion, rank-n optimised parameters:  $(a^{(n)_{opt}}, c^{(n)_{opt}})$ , with  $n=2,3$ , were obtained. In Figure 3, about 30 basins out of 450 basins are considered (for illustration) to show the series of parameters  $a_{min}$ ,  $c_{min}$  up to rank-3 basins.

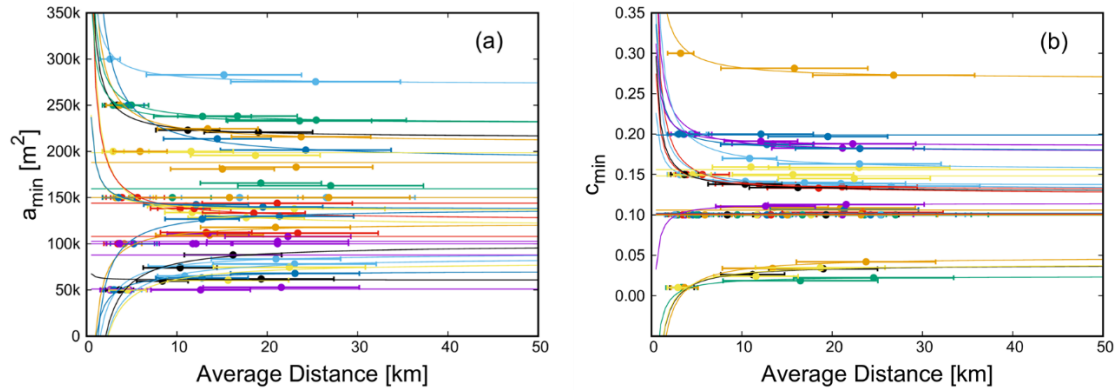


Figure 3. (a) The series of optimal parameters for  $a_{\min}$ ; (b) the series of optimal parameters in  $c_{\min}$  for domains of increasing size with increasing rank, up to rank 3. A random selection of 30 basins from 450 basins (purple in Figure 1) is made, and each curve represents one selected basin. Horizontal error bars represent the range of distances between two points within the spatial domain under consideration. The limit of large distances defines optimal values.

- iv. In the fourth step, the fit of a series of optimal values obtained from maximisation in *Step (iii)* was performed. In this work, there were two modifications in the optimisation procedure of Alvioli et al. (2020). First, to reduce the computing time, the calculations for optimised values ( $(a_{opt}^{(n)}, c_{opt}^{(n)})$ ) at the same time for all basins at rank- $n$  instead of incorporating all possible  $n$ -tuple of basins. Second, each point in Figure 3 has been weighted with a distribution distance from the centroid of the rank-1 basin.
- v. Finally, in the last step, the limiting values of each series (for each basin) were extracted, and the final SU map was delineated.

The final SU map was published as a vector layer along with a database (attribute table) of morphometric and thematic variables. Seven morphometric variables: elevation, slope, relief (elevation range), planar and tangential curvature, topographic wetness index (TWI) and vector ruggedness index (VRM) were included in the database. For each such variable, a column listing the mean value and standard deviation of the variable (calculated within each slope unit) was inserted. An additional morphometric parameter called “landforms”, defined by the geomorphons model (Jasiewicz & Stepinski, 2013) was presented in the database. A landslide inventory by Roback et al. (2017), geology and rainfall data were added as thematic variables.

### 3. Results

The final SU map is a vector layer comprising 112,674 polygons (Figure 4). The layer is embedded with an attribute table containing the planimetric area of each polygon and additional morphometric information. The average area of SUs in the map is  $0.38 \text{ km}^2$  (the minimum area is  $49,970 \text{ m}^2$ , the maximum area is  $8.03 \text{ km}^2$ , and the standard deviation is  $0.42 \text{ km}^2$ ).

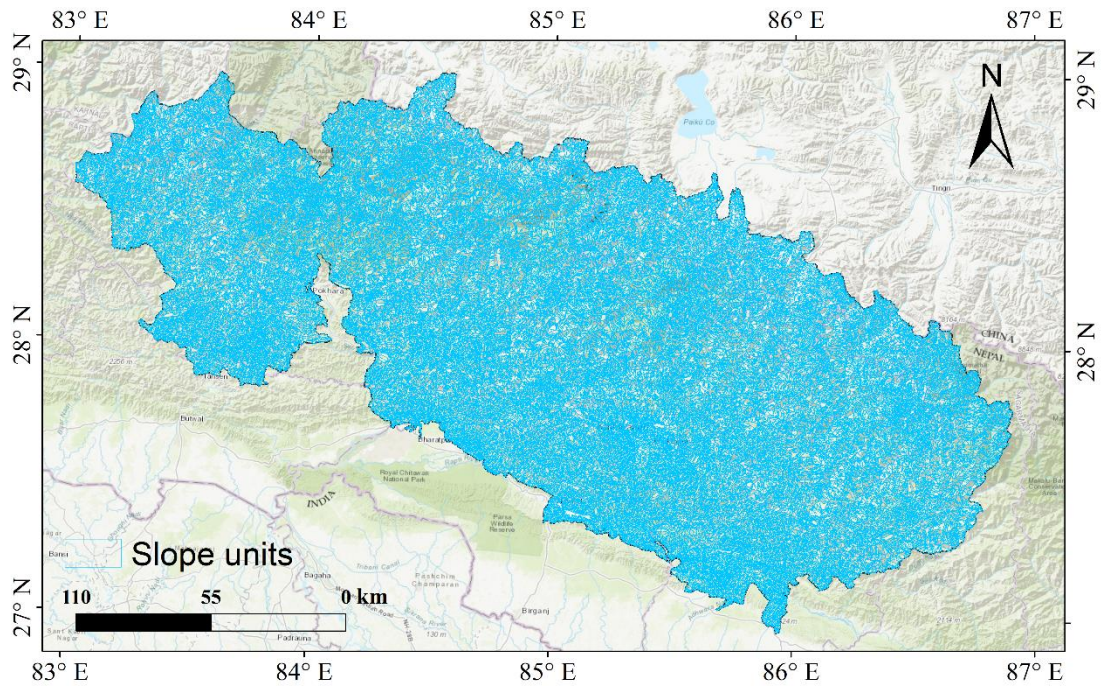


Figure 4. Slope units delineated in the study area. A zoomed-in map of a sample area is given in Figure 5.

In Figure 5, two basins with zoomed-in slope unit polygons are illustrated. Map (B) shows Langtang valley and map (C) shows a basin in the Sindhupalchowk district of Nepal.

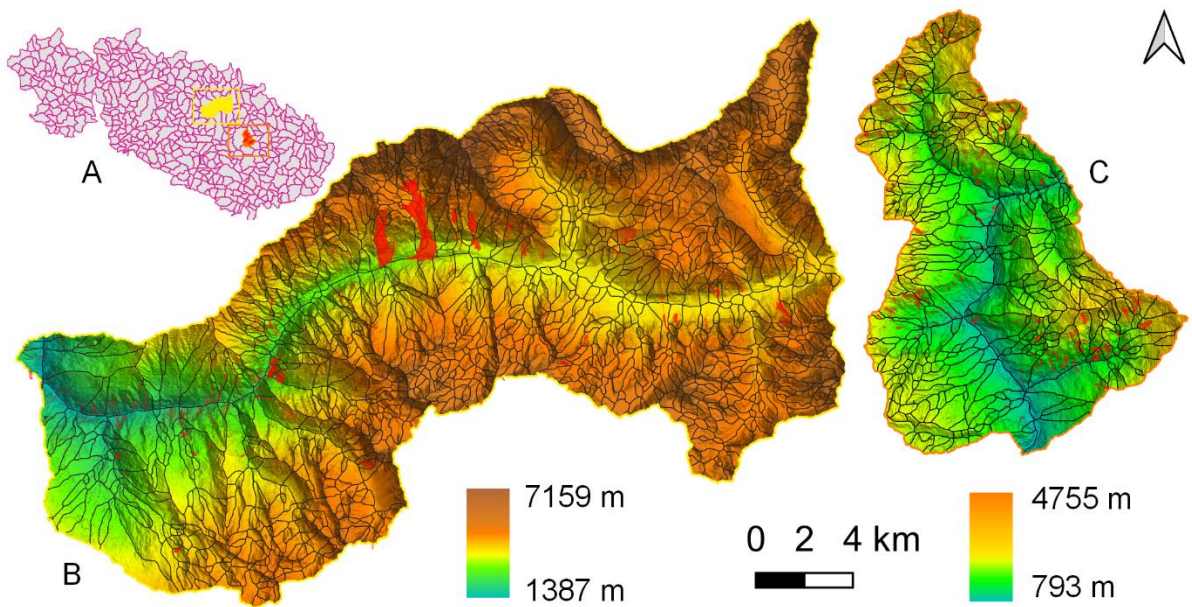


Figure 5. (A) Two sample basins were selected from the basins generated in this work; (B) the Langtang area, highlighted in yellow in (A) ; (C) the Sindhupalchowk district, highlighted in orange (C). Red polygons show earthquake-induced (B) and rainfall-induced (C) landslides.

These two regions are significant regarding the Gorkha earthquake-affected regions. One of the most destructive landslide events occurred in the Langtang Valley (Collins & Jibson, 2015),

triggering a debris avalanche that buried and killed at least 350 people (Kargel et al., 2016). Sindhupalchowk district receives intense precipitation during the monsoon season (June-September), which is why frequent rainfall-triggered landslides exist in this district. In both maps, landslides with red polygons are shown for illustrative purposes; they were induced by the earthquake in (B) and rainfall in (C).

#### **4. Contribution and future works**

The main contribution of this work is the publication of the Himalayas SU map, which was achievable with the state-of-the-art SU generation and optimisation procedure. The application of the proposed SU map is diverse.

The extent of the area covered by the map delineated for this work, consisting of about 43,000 km<sup>2</sup>, required a computationally demanding optimisation process. Therefore, the area of interest was narrowed to the Gorkha earthquake-impacted region and areas facing monsoons in central Nepal. There is a need to expand this project in the entire Himalayan belt, which is prone to mountain hazards, which is one of the future works but beyond the scope of this research.

#### **Software**

All the analyses described in this work were performed in GRASS GIS running in a Linux OS, using extensive bash scripting and parallel computing. The main slope unit delineation was performed using the *r.slopeunits* module by Alvioli et al. (2016).

#### **Map availability**

The map is available for download on the CNR-IRPI webpage: <http://geomorphology.irpi.cnr.it/tools/slope-units>.

#### **References**

- Alvioli, M., Guzzetti, F., & Marchesini, I. (2020). Parameter-free delineation of slope units and terrain subdivision of Italy. *Geomorphology*, 358, 107124. <https://doi.org/10.1016/j.geomorph.2020.107124>
- Alvioli, M., Marchesini, I., Pokharel, B., Gnyawali, K., & Lim, S. (2022). Geomorphological slope units of the Himalayas. *Journal of Maps*, 1–14. <https://doi.org/10.1080/17445647.2022.2052768>
- Alvioli, M., Marchesini, I., Reichenbach, P., Rossi, M., Ardizzone, F., Fiorucci, F., & Guzzetti, F. (2016). Automatic delineation of geomorphological slope units with *r.slopeunits* v1.0 and their optimization for landslide susceptibility modeling. *Geoscientific Model Development*, 9(11), 3975–3991. <https://doi.org/10.5194/gmd-9-3975-2016>
- Collins, B. D., & Jibson, R. W. (2015). *Assessment of Existing and Potential Landslide Hazards Resulting from the April 25, 2015 Gorkha, Nepal Earthquake Sequence (ver.1.1, August 2015)*

U.S. Geological Survey Open-file Report 2015-1142. August, 50.

<https://doi.org/10.3133/ofr20151142>

- Funk, C., Peterson, P., Landsfeld, M., Pedreros, D., Verdin, J., Shukla, S., Husak, G., Rowland, J., Harrison, L., Hoell, A., & Michaelsen, J. (2015). The climate hazards infrared precipitation with stations—a new environmental record for monitoring extremes. *Scientific Data*, 2(1), 150066. <https://doi.org/10.1038/sdata.2015.66>
- Hartmann, J., & Moosdorf, N. (2012). The new global lithological map database GLiM: A representation of rock properties at the Earth surface. *Geochemistry, Geophysics, Geosystems*, 13(12). <https://doi.org/10.1029/2012GC004370>
- Jasiewicz, J., & Stepinski, T. F. (2013). Geomorphons—a pattern recognition approach to classification and mapping of landforms. *Geomorphology*. <https://doi.org/10.1016/j.geomorph.2012.11.005>
- Kargel, J. S., Leonard, G. J., Shugar, D. H., Haritashya, U. K., Bevington, A., Fielding, E. J., Fujita, K., Geertsema, M., Miles, E. S., Steiner, J., Anderson, E., Bajracharya, S., Bawden, G. W., Breashears, D. F., Byers, A., Collins, B., Dhital, M. R., Donnellan, A., Evans, T. L., ... Young, N. (2016). Geomorphic and geologic controls of geohazards induced by Nepal's 2015 Gorkha earthquake. *Science*, 351(6269), aac8353. <https://doi.org/10.1126/science.aac8353>
- Pokharel, B., Alvioli, M., & Lim, S. (2021). Assessment of earthquake-induced landslide inventories and susceptibility maps using slope unit-based logistic regression and geospatial statistics. *Scientific Reports*, 11(1). <https://doi.org/10.1038/s41598-021-00780-y>
- Pokharel, B., Lim, S., Bhattarai, T. N., & Alvioli, M. (2023). Rockfall susceptibility along Pasang Lhamu and Galchhi-Rasuwadhi highways, Rasuwa, Central Nepal. *Bulletin of Engineering Geology and the Environment*, 82(5), 183. <https://doi.org/10.1007/s10064-023-03174-8>
- Roback, K., Clark, M. K., West, A. J., Zekkos, D., Li, G., Gallen, S. F., Champlain, D., & W, G. J. (2017). Map data of landslides triggered by the 25 April 2015 Mw 7.8 Gorkha, Nepal earthquake: US Geological survey data release. In *ScienceBase-Catalog*. <https://doi.org/https://doi.org/10.5066/F7DZ06F9>